



2019

# Quartic Metamaterials: The Inverse Method, Perturbations, and Bulk Optical Neutrality

Thomas Mulkey  
*Georgia Southern University*

Follow this and additional works at: <https://digitalcommons.georgiasouthern.edu/honors-theses>

 Part of the [Optics Commons](#)

---

## Recommended Citation

Mulkey, Thomas, "Quartic Metamaterials: The Inverse Method, Perturbations, and Bulk Optical Neutrality" (2019). *University Honors Program Theses*. 401.

<https://digitalcommons.georgiasouthern.edu/honors-theses/401>

This thesis (open access) is brought to you for free and open access by Digital Commons@Georgia Southern. It has been accepted for inclusion in University Honors Program Theses by an authorized administrator of Digital Commons@Georgia Southern. For more information, please contact [digitalcommons@georgiasouthern.edu](mailto:digitalcommons@georgiasouthern.edu).

*Quartic Metamaterials: The Inverse Method, Perturbations, and Bulk Optical Neutrality*

An Honors Thesis submitted in partial fulfillment of the requirements for Honors in the Department of Physics.

By

Thomas Mulkey

Under the mentorship of Dr. Maxim Durach

ABSTRACT

A primary goal of photonics is designing material structures that support predetermined electromagnetic field distributions. We have developed an inverse method to determine material parameters for a quartic metamaterial from six desired plane waves. This work inspired us to study how perturbations to the parameters can result in optical neutrality.

Thesis Mentor: \_\_\_\_\_

Dr. Maxim Durach

Honors Director: \_\_\_\_\_

Dr. Steven Engel

April 2019

Department of Physics

University Honors Program

**Georgia Southern University**

## Acknowledgements

I would like to thank the Blue Waters Student Internship Program and the College of Undergraduate Research for the funding provided for this project.

## Introduction

The main goal of photonics could be defined as designing material structures that support desired electromagnetic field distributions. Consider a monochromatic optical field with frequency  $\omega$  whose electric and magnetic fields are given by vector functions  $\mathbf{E}(\mathbf{r})$  and  $\mathbf{H}(\mathbf{r})$ . Creating fields in a material is contingent on the condition that the plane waves composing these fields

$$\mathbf{E}(\mathbf{r}) = \int \mathbf{E}_k \exp[i\mathbf{k}\mathbf{r}] d^3r, \quad \mathbf{H}(\mathbf{r}) = \int \mathbf{H}_k \exp[i\mathbf{k}\mathbf{r}] d^3r,$$

are supported by the material. A particular electromagnetic plane wave is allowed if it follows Maxwell's equations in  $k$ -space

$$\mathbf{k} \times \mathbf{E}_k = k_0 \mathbf{B}_k \text{ and } \mathbf{k} \times \mathbf{H}_k = -k_0 \mathbf{D}_k, \quad (1)$$

where  $k_0 = \omega/c$  and vectors  $\mathbf{D}_k = \mathbf{E}_k + 4\pi\mathbf{P}_k$  and  $\mathbf{B}_k = \mathbf{H}_k + 4\pi\mathbf{M}_k$  contain information about material response via polarization  $\mathbf{P}_k$  and magnetization  $\mathbf{M}_k$  vectors. Conventional materials correspond to dispersive, local, and isotropic material relationships  $\mathbf{D}_k = \varepsilon(\omega)\mathbf{E}_k$  and  $\mathbf{B} = \mu(\omega)\mathbf{H}$  [1]. Here we consider the implications of the most general linear local material relationship that can be expressed as [2-7]:

$$\begin{pmatrix} \mathbf{D}_k \\ \mathbf{B}_k \end{pmatrix} = \hat{M} \begin{pmatrix} \mathbf{E}_k \\ \mathbf{H}_k \end{pmatrix}, \quad \hat{M} = \begin{pmatrix} \hat{\epsilon} & \hat{X} \\ \hat{Y} & \hat{\mu} \end{pmatrix},$$

where  $\hat{\epsilon}, \hat{\mu}, \hat{X}, \hat{Y}$  are 3x3 tensors characterizing dielectric permittivity, magnetic permeability and magnetoelectric coupling correspondingly. This includes 36 effective material parameters, which populate the 6x6 transformation matrix  $\hat{M}$  (see numerical example in Fig. 1(a)). Here we use a linear relationship between the pairs D, B and E, H (see Ref. [1]), but other equivalent choices could be considered more natural for the reasons of relativistic invariance, which we do not discuss here (see Ref. [7,8]).

In this paper, we demonstrate that one needs to specify the  $k$ -vectors and  $\mathbf{E}_k, \mathbf{H}_k$  amplitudes of 6 arbitrary plane waves (with some limitations specified below) to fully define the required 36 material parameters of the material that will support these waves and, correspondingly, all the other fields possible in the bulk of this material. Here we do not discuss the immediate availability with the current technology of the values of material parameters we obtain in our examples but provide a recipe to obtain the values of the parameters needed for the desired field distributions to inform and drive the future design of the corresponding metamaterials. The interest in metamaterials with extreme and unconventional properties [9], such as negative refraction, hyperbolic dispersion, optical magnetism, anisotropy, chirality, cloaking, supercoupling, non-reciprocity etc. is growing to feed the technological demands of the industries, marketplaces and security [10-11].

Usually one starts with a set of the effective material parameters for a material or metamaterial at hand and finds the possible electromagnetic fields in this material (the direct problem in Fig. 1). Maxwell's equations (1) can be rewritten as  $\hat{Q}\Gamma = \hat{M}\Gamma$ , with  $\Gamma = (E_x, E_y, E_z, H_x, H_y, H_z)$  and

$$\hat{M} = \begin{pmatrix} \hat{\epsilon} & \hat{X} \\ \hat{Y} & \hat{\mu} \end{pmatrix}, \hat{Q} = \begin{pmatrix} 0 & -\hat{R} \\ \hat{R} & 0 \end{pmatrix}, \hat{R} = \frac{1}{k_0} \begin{pmatrix} 0 & -k_z & k_y \\ k_z & 0 & -k_x \\ -k_y & k_x & 0 \end{pmatrix}.$$

This system has nontrivial solutions if its determinant of matrix  $\hat{\Delta} = \hat{M} - \hat{Q}$  is zero

$$\begin{aligned} \text{Det}(\hat{\Delta}) &= \text{Det} \left( \hat{\epsilon} - (\hat{X} + \hat{R})\hat{\mu}^{-1}(\hat{Y} - \hat{R}) \right) \text{Det}(\hat{\mu}) \\ &= \text{Det} \left( \hat{\mu} - (\hat{Y} - \hat{R})\hat{\epsilon}^{-1}(\hat{X} + \hat{R}) \right) \text{Det}(\hat{\epsilon}) = 0. \end{aligned} \quad (2)$$

The determinant (2) is a multivariate quartic function  $f = f(k_x, k_y, k_z)$ , i.e. it is a polynomial of degree 4. In other words, the  $k$ -vectors of the plane waves that satisfy Maxwell's equations belong to a quartic surface  $f(k_x, k_y, k_z) = 0$  in  $k$ -space (see example in Fig. 1(b)) [3,12-16]. Each point on such a photonic quartic surface corresponds to a solution of Eq. (1), i.e. to a field vector  $\Gamma = (E_x, E_y, E_z, H_x, H_y, H_z)$ . The quartic surfaces we considered correspond to the following equation

$$\sum_{i+j+l+m=4} [\alpha_{ijlm} k_x^i k_y^j k_z^l k_0^m] = 0 \quad (3)$$

with 35 coefficients  $\alpha_{ijlm}$ . In the sum the powers  $i, j, l, m$  run from 0 to 4 such that  $i + j + l + m = 4$ .

Mathematically, there is no complete classification or global picture of quartic surfaces. In the case of singular quartics, the essential properties of surfaces with nodes (or nodal curves) are discussed in Ref [17]. A special case of (mildly singular) quartic K3 surfaces correspond to Kummer varieties. These K3 surfaces have the property that they can be seen as the quotient of two tori by an involution having 16 fixed points. The relation between Kummer K3s and the optics of the studied materials has been discussed in Refs. [3,6].

Smooth quartic surfaces are a classical example of K3 surfaces. Their fundamental group is trivial and their canonical class as well. Quartic K3 surfaces are parametrized by 19 moduli (essentially, coefficients). K3 surfaces are very interesting as their properties combine geometric and arithmetic features [18]. Nevertheless, some families of smooth quartic surfaces, such as ruled quartics, have been studied and classified before [19].

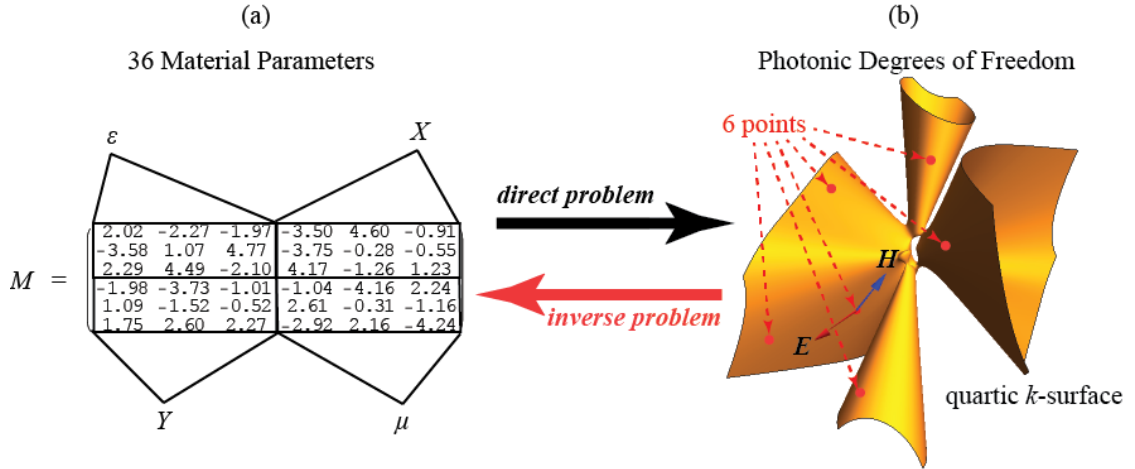


Fig. 1. The direct and inverse problems of quartic photonics. (a) a numerical example of the effective material parameters matrix  $\hat{M}$ ; (b) the corresponding quartic surface in  $k$ -space with 6 points selected for the inverse problem; vector amplitudes of the electric (red) and magnetic (blue) fields are shown for one of the points.

### The Inverse Problem

The coefficients  $\alpha_{ijklm}$  of the quartic surface Eq. (3) can be explicitly found from the material parameters using Eq. (2). But for the design of the metamaterials, it would be interesting to solve the inverse problem, i.e. to find the effective material parameters of the metamaterials that would support specific plane waves needed for the creation of desired field distributions. In general, the coefficients  $\alpha_{ijklm}$  in Eq. (3) are complicated nonlinear functions of the material parameters which cannot be easily inverted to resolve the inverse

problem of finding material parameters starting from the desired shape of the quartic surface, even though this has been done in the simple cases which deal with the spherical k-surface [20,21], and k-surface composed of two shells [22,23]. In any case, the knowledge of all  $\alpha_{ijlm}$  is not the full solution of the direct problem, since it does not contain the information about the field vectors  $\Gamma$  of the supported waves. Therefore, the coefficients  $\alpha_{ijlm}$  should not be the input information of the inverse problem.

We formulate the inverse problem (see Fig. 1) as follows. Imagine one needs to create a metamaterial that propagates a set of desired plane waves whose  $k$ -vectors as well as the field vectors  $\Gamma = (E_x, E_y, E_z, H_x, H_y, H_z)$  are given. These plane waves should satisfy Eqs. (1) with the effective material parameters in the unknown matrix  $\widehat{M}$ . Since we have 36 unknown material parameters, we can specify characteristics of 6 plane waves to form a complete system of equations.

We rewrite Eqs. (1) for the 6 desired waves simultaneously as a matrix equation  $\widehat{M}\widehat{G} = \widehat{P}$ , where

$$\widehat{G} = \begin{pmatrix} E_{x1} & E_{x2} & E_{x3} & E_{x4} & E_{x5} & E_{x6} \\ E_{y1} & E_{y2} & E_{y3} & E_{y4} & E_{y5} & E_{y6} \\ E_{z1} & E_{z2} & E_{z3} & E_{z4} & E_{z5} & E_{z6} \\ H_{x1} & H_{x2} & H_{x3} & H_{x4} & H_{x5} & H_{x6} \\ H_{y1} & H_{y2} & H_{y3} & H_{y4} & H_{y5} & H_{y6} \\ H_{z1} & H_{z2} & H_{z3} & H_{z4} & H_{z5} & H_{z6} \end{pmatrix}$$

is the matrix whose columns are vectors  $\Gamma_i$ , while columns of matrix  $\widehat{P}$  are vectors  $\widehat{Q}_i\Gamma_i$ , where  $i$  runs from 1 to 6. The antisymmetric matrix  $\widehat{Q}_i$  is composed from the  $k$ -vector components, while  $\Gamma_i$  from fields of the 6 desired waves. Now this system can be solved,

and the effective material parameters matrix can be found explicitly from the parameters of the 6 chosen waves

$$\hat{M} = \hat{P}\hat{G}^{-1} \quad (4)$$

Finding matrix  $\hat{M}$  with the unknown material parameters gives the solution to the problem of finding a metamaterial that supports a desired field distribution (i.e. the inverse problem in Fig. 1).

### **Quasistatic High-K Limit**

Hyperbolic metamaterials, a class of “quadratic” metamaterials (i.e. their k-surfaces – or iso-frequency/Fresnel surfaces [24] - are described by quadratic equations), have generated huge interest, since they support high-k plane waves, a property which leads to diverging photonic density of states allowing spontaneous and thermal emission engineering [25-28].

In the quartic metamaterials Eqs. (2)-(3) may have asymptotic solutions with large  $k = \sqrt{k_x^2 + k_y^2 + k_z^2} \gg k_0$  as well. In this asymptotic limit only the 4th order terms with  $m = 0$  in Eq. (3) matter.

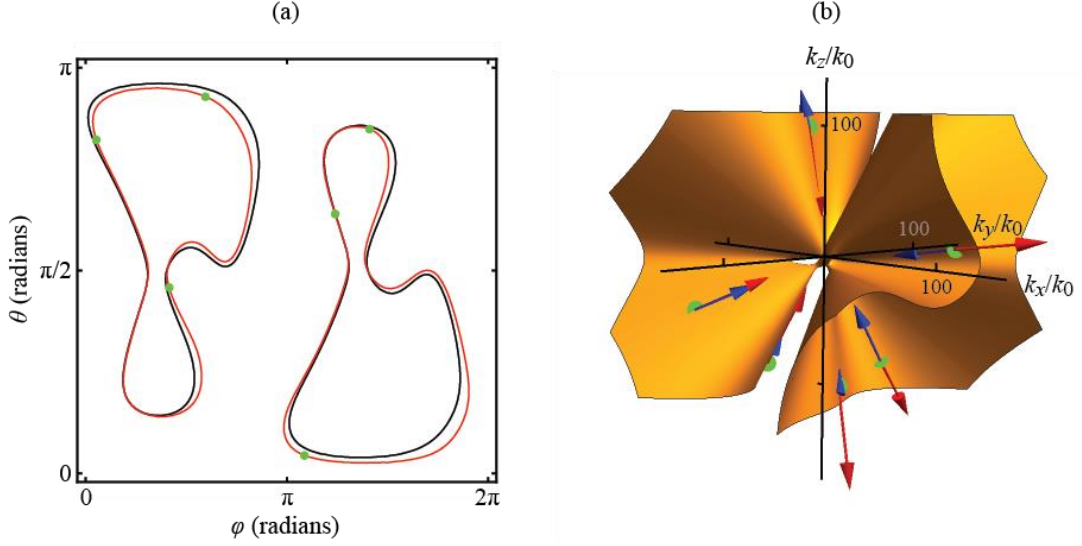


Fig. 2. Numerical example of asymptotic behavior. (a) asymptotic  $k$ -surface in  $(\varphi, \theta)$  coordinates (black) compared to  $k = 100k_0$  cross-section (red); green points are selected at this cross-section for effective material parameters retrieval; (b) the corresponding quartic surface in  $k$ -space with the same green points indicated with vector amplitudes of electric (red) and magnetic (blue) fields. Note that the fields are practically parallel to the  $k$  vectors as they should in the high- $k$  quasistatic limit.

When considering the asymptotic behaviour of a quartic  $k$ -surface, one can intersect the quartic surface with a sphere of radius  $k$  and look at the behavior in the limit  $k \gg k_0$ . Consider a spherical coordinate system in  $k$ -space  $k_x = k \sin \theta \sin \varphi$ ,  $k_y = k \sin \theta \cos \varphi$ ,  $k_z = k \cos \theta$ . In this coordinate system Eq. (3) in the limit  $k \gg k_0$  asymptotically reads

$$\sum_{i+j+l=4} [\alpha_{ijl0} (\sin \theta \sin \varphi)^i (\sin \theta \cos \varphi)^j (\cos \theta)^l] = 0 \quad (5)$$

The solution of Eq. (5) is a function  $f_{as}(\theta, \varphi)$  which gives directions in  $k$ -space corresponding to asymptotic solutions of Eqs. (2)-(3). For example, the topology of the  $k$ -surface of a hyperbolic material in the asymptotic limit corresponds to two circles in the limit  $k \gg k_0$ . The more general class of quartic metamaterials provides opportunity to engineer the high- $k$  states. To classify the quartic  $k$ -surfaces in the asymptotic limit

topologically it is convenient to use the projective plane  $P^2$ . The classification follows from theorem [29]: A *smooth projective real* quartic curve consists *topologically* of: (i) 1 circle; (ii) 2 adjacent circles (example in Fig. 2 or hyperbolic materials); (iii) 2 nested circles; (iv) 3 circles; (v) 4 circles (example in Fig. 1); (vi) an empty set (e.g. vacuum).

We show how our solution to the inverse problem applies to the engineering of the high- $k$  behavior. For illustration, we start with a randomly chosen effective material parameters matrix

$$\hat{M} = \begin{pmatrix} -3.15 & 4.81 & 4.47 & -1.66 & -0.52 & -2.18 \\ -2.82 & 2.81 & 0.17 & 2.74 & -3.71 & 1.06 \\ -1.55 & 1.60 & 0.38 & -0.56 & -4.37 & -0.66 \\ -2.29 & 4.24 & -2.95 & -2.23 & 3.68 & -4.43 \\ -3.30 & 4.22 & -2.06 & -0.98 & 4.51 & 1.00 \\ 2.96 & -4.58 & 1.23 & -3.31 & -2.70 & 4.19 \end{pmatrix}. \quad (6)$$

Solving Eqs. (1)-(2) we arrive at the quartic surface shown in Fig. 2. In Fig. 2(a) we show a cross-section of this surface at  $k = 100 k_0$  (red curve) and the corresponding asymptotic solution  $f_{as}(\theta, \varphi)$  of Eq. (5) (black). From this high- $k$  cross-section, 6 points are randomly selected, shown in green in both panels Fig. 2(a) and (b). In Fig. 2(b), the quartic surface is plotted in Cartesian coordinates with the selected 6 points and the corresponding field amplitudes shown by arrows (electric fields are red, magnetic – blue). Retaining the data of only the selected 6 points, we solve Eq. (4) and get the parameters of matrix (6) back exactly, with no deviation. The field vectors in Fig. 2(b) show a major property of the high- $k$  quasistatic electromagnetic fields. Both electric and magnetic fields are directed with high precision in the radial direction, i.e. they are parallel to the  $k$ -vectors  $\mathbf{E}, \mathbf{H} \parallel \mathbf{k}$ .

## Isotropic Materials

As a further example of how our method works we apply it to the waves with  $\mathbf{k}_1 = k_1 \hat{\mathbf{x}}$ ,  $\mathbf{k}_2 = k_2 \hat{\mathbf{y}}$ ,  $\mathbf{k}_3 = k_3 \hat{\mathbf{z}}$ ,  $\mathbf{k}_4 = -k_4 \hat{\mathbf{x}}$ ,  $\mathbf{k}_5 = -k_5 \hat{\mathbf{y}}$ ,  $\mathbf{k}_6 = -k_6 \hat{\mathbf{z}}$ , and polarizations given by

$$\hat{G} = \begin{pmatrix} 0 & 0 & E_3 & 0 & E_5 & 0 \\ E_1 & 0 & 0 & 0 & 0 & E_6 \\ 0 & E_2 & 0 & E_4 & 0 & 0 \\ 0 & H_2 & 0 & 0 & 0 & H_6 \\ 0 & 0 & H_3 & H_4 & 0 & 0 \\ H_1 & 0 & 0 & 0 & H_5 & 0 \end{pmatrix}$$

The resulting matrix  $\hat{M}$  obtained using Eq. (4) has off diagonal elements of the form

$$M_{12} = \frac{E_2 H_1 H_4 H_5 (E_5 H_3 k_3 - E_3 H_5 k_5)}{E_1 E_2 E_3 H_4 H_5 H_6 - H_1 H_2 H_3 E_4 E_5 E_6},$$

which all become zero in the respective limits  $H_3 \rightarrow E_3$ ,  $H_5 \rightarrow E_5$ ,  $k_3 \rightarrow k_5$ . The diagonal elements are of the form

$$M_{11} = \frac{H_3 H_5 (E_1 E_2 H_4 H_6 k_3 - E_4 E_6 H_1 H_2 k_5)}{E_1 E_2 E_3 H_4 H_5 H_6 - H_1 H_2 H_3 E_4 E_5 E_6},$$

which all become 1 in the limits  $k_i \rightarrow k_0 E_i / H_i$ . In other words, for the plane wave propagation characteristic of vacuum we obtain vacuum unit matrix  $\hat{M} = \hat{1}$ .

Generally, in isotropic materials the  $k$ -surfaces are quadratic and correspond to pairs of spheres, topological features of which were studied in Ref. [30]. In a direction  $(\theta, \varphi)$  in  $k$ -space there are 2 waves propagating in isotropic medium with 2 different polarization. There are 2 more waves in the opposite direction (see Fig. 3(a)).

## Quartic Metamaterials

Such polarization separation and quadratic property disappears in quartic media. After fixing  $(\theta, \varphi)$  Eqs. (2)-(3) take the form

$$\sum_{i+j+l+m=4} \left[ \alpha_{ijlm} (\sin \theta \sin \varphi)^i (\sin \theta \cos \varphi)^j (\cos \theta)^l \left( \frac{k}{k_0} \right)^{4-m} \right] = 0. \quad (7)$$

Eq. (7) is a single-variable quartic equation with respect to  $k/k_0$ , which in general has up to 4 roots representing 4 different plane waves propagating in the direction  $(\theta, \varphi)$ . From this a fundamental limitation follows that one cannot require all 6 waves in the inverse problem to have parallel  $k$ -vectors.

Nevertheless, we can select any 4 values of the  $k$ -number in any direction and 2 more in other directions. As an example, we were able to obtain a quartic material (Fig. 4(b), “reindeer Rudolph”  $k$ -surface) with the following effective parameters matrix:

$$\hat{M} = \begin{pmatrix} -4.34 & 3.11 & 10.63 & 5.57 & 3.41 & -10.10 \\ -0.50 & 0.04 & -3.81 & -1.24 & 1.98 & 1.56 \\ 3.45 & -2.77 & -12.72 & 1.27 & 0.93 & -1.16 \\ 1.97 & -5.38 & 2.63 & -5.12 & -2.14 & -0.55 \\ 4.48 & -3.82 & -3.78 & -2.42 & -0.90 & 0.19 \\ -0.26 & -0.79 & 0.89 & -1.18 & -0.15 & 0.90 \end{pmatrix}. \quad (8)$$

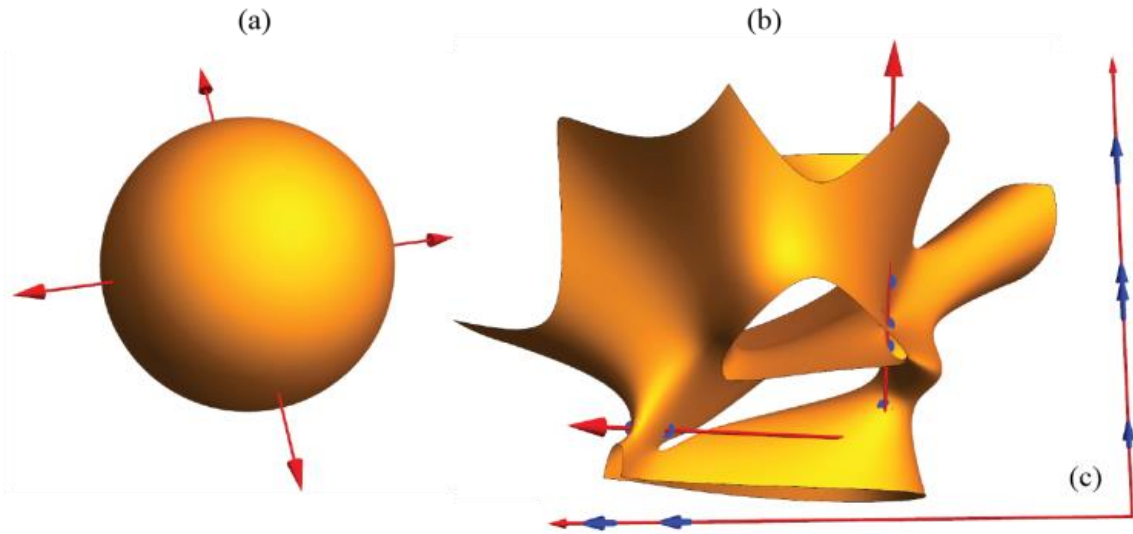


Fig. 3. k-surface engineering; (a) k-surface of an isotropic material; a line in any direction intersects 2 states; (b)-(c) “reindeer Rudolph” k-surface features extremely non-reciprocal behavior, with  $k$ -vectors (b) and Poynting vectors (c) of 4 states pointing in the same direction.

In this material all 4 plane waves with  $(\theta, \varphi) = (0.11\pi, 1.71\pi)$  have wave-vectors which point in the same direction and there are no waves with opposite  $k$ -vectors (Fig. 3(b)). Note that directions of the  $k$ -vectors correspond to the direction of the phase propagation. We were able to select the field vectors  $\Gamma_i$  such that the Poynting vectors for the 6 waves point in the same directions as  $k$ -vectors [Poynting vectors for the waves in Fig 3(b) are shown in Fig. 3(c)]. This means we were able to design all 4 waves in a direction  $(\theta, \varphi)$  to propagate both energy and phase in this direction - an example of extreme non-reciprocity [2,31-34].

In some cases, the metamaterials are subject to restrictions, e.g. if some of the effective material parameters are known *a priori*. In such situations one could require existence of less than 6 waves and complement the truncated Eqs. (4) with extra restrictions on material parameters. For example, one could require existence of 3 specific waves in a metamaterial

and matrices  $\hat{G}$  and  $\hat{P}$  in Eq. (4) would have 3 columns instead of 6. Then Eq. (4) are rewritten as

$$\hat{\epsilon} = -\hat{P}_H \hat{E}^{-1} - \hat{X} \hat{H} \hat{E}^{-1}, \quad \hat{\mu} = \hat{P}_E \hat{H}^{-1} - \hat{Y} \hat{E} \hat{H}^{-1}, \quad (9)$$

i.e. the permittivity and permeability matrices  $\hat{\epsilon}$  and  $\hat{\mu}$  can be expressed via the matrices  $\hat{X}$  and  $\hat{Y}$ ,  $k$ -vectors of the selected waves and the amplitudes of their fields in the matrices

$$k_0 \hat{P}_E = (\mathbf{k}_1 \times \mathbf{E}_1, \mathbf{k}_2 \times \mathbf{E}_2, \mathbf{k}_3 \times \mathbf{E}_3)$$

$$k_0 \hat{P}_H = (\mathbf{k}_1 \times \mathbf{H}_1, \mathbf{k}_2 \times \mathbf{H}_2, \mathbf{k}_3 \times \mathbf{H}_3)$$

$$\hat{E} = \begin{pmatrix} E_{x1} & E_{x2} & E_{x3} \\ E_{y1} & E_{y2} & E_{y3} \\ E_{z1} & E_{z2} & E_{z3} \end{pmatrix} \text{ and } \hat{H} = \begin{pmatrix} H_{x1} & H_{x2} & H_{x3} \\ H_{y1} & H_{y2} & H_{y3} \\ H_{z1} & H_{z2} & H_{z3} \end{pmatrix}.$$

The inspection of the modified inverse solution of the photonic problem given by Eqs. (9) leads to the conclusion that if the magnetoelectric coupling  $\hat{X}$  and  $\hat{Y}$  is fixed one can freely select only 3 plane waves. Eqs (9) are particularly convenient for the design of materials in absence of magnetoelectric coupling  $\hat{X} = \hat{Y} = \hat{0}$  in which case  $\hat{\epsilon} = -\hat{P}_H \hat{E}^{-1}$ ,  $\hat{\mu} = \hat{P}_E \hat{H}^{-1}$ .

### Complex Bi-Anisotropic Parameters

In another example we apply Eqs. (9) as shown in Fig. 4 where the magnetoelectric coupling has a chiral form  $\hat{X} = -\hat{Y} = -i\hat{1}$  and the medium supports 3 of the 6 waves selected for Fig. 3(b-c). This is an example of a situation, when matrix  $\hat{M}$  is complex

$$\text{Re}[\widehat{M}] = \begin{pmatrix} 18.6 & -15.4 & -18.2 & 0 & 0 & 0 \\ 2.41 & -1.48 & 7.94 & 0 & 0 & 0 \\ 7.21 & -6.01 & -16.3 & 0 & 0 & 0 \\ 0 & 0 & 0 & 2.34 & 2.59 & 3.73 \\ 0 & 0 & 0 & -1.00 & 0.24 & -1.13 \\ 0 & 0 & 0 & 0.62 & 0.86 & 2.18 \end{pmatrix}. \quad (10a)$$

$$\text{Im}[\widehat{M}] = \begin{pmatrix} -0.39 & -0.23 & -2.56 & -1 & 0 & 0 \\ 2.52 & -1.78 & 2.52 & 0 & -1 & 0 \\ -1.64 & 1.11 & 2.29 & 0 & 0 & -1 \\ 1 & 0 & 0 & 1.31 & 0.44 & 0.97 \\ 0 & 1 & 0 & 1.88 & 0.97 & 1.03 \\ 0 & 0 & 1 & 0.02 & -0.15 & -0.24 \end{pmatrix} \quad (10b)$$

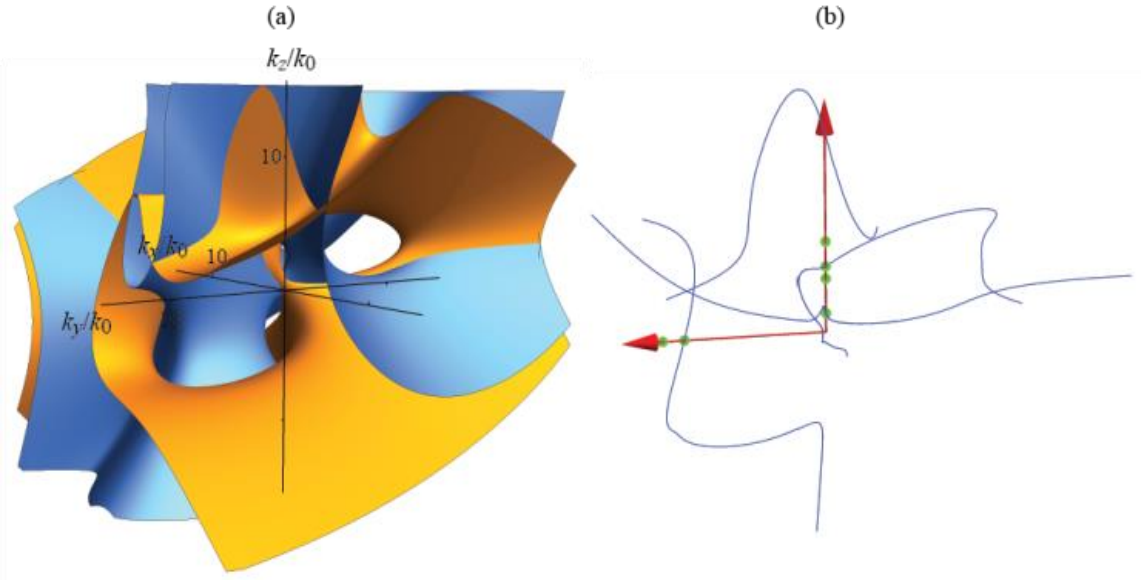


Fig. 4.  $k$ -surface with complex material parameters. (a) Two quartic surfaces with coefficients  $\text{Re}[\alpha_{ijlm}]$  (orange) and  $\text{Im}[\alpha_{ijlm}]$  (blue); (b) the intersection of the quartic surfaces of panel (a) shown as blue curve of solutions of Eqs. (2)-(3). The desired 3 waves are highlighted in green and belong to the curve.

If matrix  $\widehat{M}$  is complex the coefficients  $\alpha_{ijlm}$  in Eq. (3) are complex too and Eqs. (2)-(3) correspond to two quartic surfaces with coefficients  $\text{Re}[\alpha_{ijlm}]$  and  $\text{Im}[\alpha_{ijlm}]$  (orange and blue in Fig. 4(a)). The solutions of Eqs. (2)-(3) with real  $k_0$  and  $\mathbf{k}$  are at the intersection of

these quartic surfaces which is a curve in  $k$ -space (blue in Fig. 4(b)). It is interesting to compare the complex bi-anisotropic metamaterial shown in Fig. 4(b) to similar and connected problems of “extreme materials” considered in Ref. [35] from the "forward" instead of "inverse" point of view.

One can see how the solution curve passes through the desired 3 waves (3 of the 6 waves highlighted in green in Fig. 4(b) and blue in Fig. 3(b)). Note that the solution vectors  $\Gamma_i$  for the selected 3 waves are the same as in the case of the “reindeer Rudolph”  $k$ -surface in Fig. 3(b-c), i.e. they are real and represent linear polarization, in contrast with the isotropic chiral materials where solution vectors are complex, representing circular polarization.

### **Perturbations and Bulk Optical Neutrality**

Following the work on quartic metamaterials and their  $k$ -surfaces, we became interested on how the  $k$ -surface responds to perturbations in the material parameters matrix  $\hat{M}$ . The material of choice to be perturbed was a vacuum with elements  $M_{ij} = \{1, i = j; 0, i \neq j\}$ . The vacuum was perturbed by adding a matrix  $\hat{P}$  with elements  $P_{ij}$ . Maxwell’s equations now have the form  $\hat{Q}\Gamma = (\hat{M} + \hat{P})\Gamma$ . This can be further reduced to

$$(-\hat{Q} + \hat{M} + \hat{P})\Gamma = \Delta\Gamma = 0 \quad (11)$$

Nontrivial solutions to Equation (11) exist when the determinant of  $\Delta$  is equal to zero, and the resulting function is the  $k$ -surface. For  $\hat{P} = \hat{0}$ , the  $k$ -surface is that of a vacuum, two overlapping spheres of radius 1 centered about the origin.

$$(-1 + k_x^2 + k_y^2 + k_z^2)^2 = 0 \quad (12)$$

For arbitrary  $P_{ij}$ , the determinant of  $\Delta$  becomes quite complex. The function can be simplified by assuming the perturbations are sufficiently small in magnitude,  $|P_{ij}| \ll 1$ , and the dominant terms are those linear with respect to the perturbation elements. Under this approximation the k-surface is described by the following:

$$\begin{aligned} & (-1 + k_x^2 + k_y^2 + k_z^2) \left( -1 + Ak_x + k_x^2 + H(-1 + k_x^2) + Ek_y + Bk_xk_y + k_y^2 + \right. \\ & \left. J(-1 + k_y^2) + Fk_z + Ck_xk_z + Gk_yk_z + k_z^2 + K(-1 + k_z^2) \right) = 0 \end{aligned} \quad (13)$$

The nine undefined coefficients of eq. (13) are dependent solely on the values of elements  $P_{ij}$ , and can be found in Table A.

Immediately, several notable items can be seen. First, under the linear perturbation approximation, one sphere remains unperturbed from its original in the vacuum. Second, the nine undefined coefficients are independent from six of the perturbation elements:  $P_{14}, P_{25}, P_{36}, P_{41}, P_{52}$ , and  $P_{63}$ . Under the linear perturbation approximation, these six elements can hold any value and not impact the resulting perturbed k-surface. Lastly, if the nine coefficients are set to zero, the k-surface will reduce to be identical to that of the unperturbed vacuum, eq. (12). This indicates the perturbed vacuum would be optically neutral with respect to the unperturbed vacuum. Optical neutrality is an area of research that is gaining interest with developments in producing invisibility in the absence of the traditional cloak [37] and neutral inclusion, in which the effective permittivity is unity [38].

We now wish to establish a set of rules to select  $\hat{P}$  to guarantee an optically neutral result. Here, we also restrict ourselves to reciprocal materials. A material is considered reciprocal if  $\hat{M}$  follows three conditions:  $\hat{\epsilon} = \hat{\epsilon}^T$ ,  $\hat{\mu} = \hat{\mu}^T$ , and  $\hat{X}^T = -\hat{Y}$ .

From the reciprocal conditions, coefficients A, E, and F are equal to zero regardless of the values for their constituent elements  $P_{ij}$ . Furthermore, coefficients the remaining six coefficients can be reduced to the form

$$P_{ij} = -P_{kl},$$

where elements  $P_{ij}$  are the perturbation elements applied to  $\hat{\epsilon}$  and elements  $P_{kl}$  are perturbation elements applied to  $\hat{\mu}$ . From this, a new condition is established:

$$\hat{\epsilon} - \hat{I} = -(\hat{\mu} - \hat{I}),$$

where  $\hat{I}$  represents the unity matrix. Applying the new condition in conjunction with the reciprocity conditions to  $\hat{P}$  yields a perturbation matrix resulting in no changes to the k-surface when applied to a vacuum. These perturbations have the form

$$\hat{P} = \begin{pmatrix} p_{11} & p_{12} & p_{13} & p_{14} & p_{15} & p_{16} \\ p_{12} & p_{22} & p_{23} & p_{24} & p_{25} & p_{26} \\ p_{13} & p_{23} & p_{33} & p_{34} & p_{35} & p_{36} \\ -p_{14} & -p_{24} & -p_{34} & -p_{11} & -p_{12} & -p_{13} \\ -p_{15} & -p_{25} & -p_{35} & -p_{12} & -p_{22} & -p_{23} \\ -p_{16} & -p_{26} & -p_{36} & -p_{13} & -p_{23} & -p_{33} \end{pmatrix}.$$

### A Note on Polarizations

We have shown that the k-surface of the material resulting from perturbation is identical to that of a vacuum under certain approximations. This indicates the k-vectors and field amplitudes at a given point on the k-surface are identical, but this does not reveal if the polarizations have been unaltered by the perturbations. To better study the impact on polarizations, we reformulate the problem as an eigenvalue problem. We begin with Maxwell's equations with the perturbation in matrix form

$$\hat{Q}\Gamma = k_0(\hat{M} + \hat{P})\Gamma \quad (13).$$

Previously, we subtracted the matrices  $\hat{Q}$  and  $\hat{M}$ , but instead we will write it as  $(\hat{M} + \hat{P})^{-1}\hat{Q}\Gamma = k_0\Gamma$ . A simple manipulation allows us to write

$$((\hat{M} + \hat{P})^{-1}\hat{Q} - k_0\hat{I})\Gamma = 0 \quad (14),$$

where  $\hat{I}$  is the unity matrix. The problem stated in eqn. 14 is now in the form of an eigenvalue problem and can be solved as such. The characteristic polynomial is given by the determinant of  $(\hat{M} + \hat{P})^{-1}\hat{Q} - k_0\hat{I}$  whose roots are the eigenvalues. The eigenvectors associated with these roots represent the polarizations of the plane waves supported by the perturbed material. This alternative approach allows for easier inspection of polarizations on the perturbed metamaterial.

## Conclusion

In summary, we have established a method for the inverse problem of photonics allowing for the effective material parameters of the metamaterial to be determined from a known set of plane wave k-vectors and fields. Furthermore, we have studied the impact of small perturbations on the material parameters of a vacuum and devised a set of conditions in which the resulting material is optically neutral with respect to the vacuum.

## Citations

1. L. D. Landau, E. M. Lifshitz and L. P. Pitaevskii, *Electrodynamics of continuous media*. Vol. 8, (Elsevier, 2013).
2. A. Sihvola, *Metamaterials in electromagnetics*, *Metamaterials* 1, pp. 2–11, (2007).
3. P. Baekler, A. Favaro, Y. Itin, F.W. Hehl, The Kummer tensor density in electrodynamics and in gravity. *Annals of Physics*, 349, pp.297-324 (2014).
4. F. W. Hehl, Yu. N. Obukhov, J. -P. Rivera and H. Schmid, Relativistic nature of a magnetoelectric modulus of Cr<sub>2</sub>O<sub>3</sub> crystals: A fourdimensional pseudoscalar and its measurement, *Phys. Rev. A* 77, p. 022106 (2008)
5. I.V. Lindell, A.H. Sihvola, S.A. Tretyakov, A.J. Viitanen, *Electromagnetic Waves in Chiral and Bi-isotropic Media* (Artech House, Norwood, MA, 1994).
6. A. Serdyukov, I. Semchenko, S. Tretyakov, A. Sihvola, *Electromagnetics of Bi-anisotropic Materials: Theory and Applications*. (Gordon and Breach, Amsterdam, 2001).
7. F. W. Hehl and Yu. N. Obukhov, *Foundations of Classical Electrodynamics: Charge, flux, and metric* (Birkhauser, Boston, 2003)
8. E.J. Post, *Formal Structure of Electromagnetism*, Dover, Mineola, NY (1995)
9. Sihvola, A., S. Tretyakov, and A. De Baas. "Metamaterials with extreme material parameters." *Journal of Communications Technology and Electronics* 52, no. 9 (2007): 986-990.
10. M. A. Noginov, and V. A. Podolskiy, eds. *Tutorials in metamaterials* (CRC press, 2011).
11. M. A. Noginov, G. Dewar, M. W. McCall, and N. I. Zheludev, *Tutorials in complex photonic media*, SPIE, 2009.
12. I.V. Lindell, *Plane-Wave Propagation in Electromagnetic PQ Medium*, *Progress In Electromagnetics Research*, Vol. 154, pp.23-33 (2015).
13. K. A. Vytovtov, "Investigation of the plane wave behavior within bianisotropic media." In *Mathematical Methods in Electromagnetic Theory*, Vol. 1, pp. 326-328 (2000).
14. Favaro et al., *Phys. Rev. A* 93, no. 1, 013844 (2016), arXiv:1510.05566.
15. A.B. Balakin et al., "Non-minimal Einstein-Maxwell theory: the Fresnel equation and the Petrov classification of a trace-free susceptibility tensor," arXiv:1710.08013
16. A. Favaro, "Electromagnetic wave propagation in metamaterials: a visual guide to Fresnel-Kummer surfaces and their singular points." In 2016 URSI International Symposium on Electromagnetic Theory (EMTS), (pp. 622-624). IEEE, 2016
17. Jessop, C. *Quartic Surfaces with Singular Points*. Cambridge University Press, 1916
18. D. Huybrechts, *Lectures on K3 surfaces*, Vol. 158. Cambridge University Press, 2016.
19. K. Rohn, "Die verschiedenen Arten der Regelflächen vierter Ordnung", (1886). *Mathematische Abhandlungen aus dem Verlage Mathematischer Modelle von Martin Schilling*. Halle a. S., 1904. *Mathematische Annalen*, vol. 28, No. 2, pp. 284–308 (1886)
20. [2] A. Favaro and L. Bergamin, The non-birefringent limit of all linear, skewonless media and its unique light-cone structure. *Ann. Phys. (Berlin)*, volume 523, issue 5, pages 383–401, 2011.
21. [3] M.F. Dahl, Determination of an electromagnetic medium from the Fresnel surface. *J. Phys. A: Math. Theor.*, volume 45, 405203, 2012.
22. [4] M.F. Dahl, Non-dissipative electromagnetic media with two Lorentz null cones. *Ann. Phys. (NY)*, volume 330, pages 55–73, 2013.
23. [5] M.F. Dahl, Characterisation and representation of non-dissipative electromagnetic medium with two Lorentz null cones. *J. Math. Phys.*, volume 54, 011501, 2013.
24. Kiehn et al., *Phy.Rev.A* 43, 5665 (1991)
25. Z. Jacob, I. Smolyaninov, E. Narimanov. "Broadband Purcell effect: Radiative decay engineering with metamaterials." *Applied Physics Letters* 100 (18), p. 181105 (2012)
26. M. A. Noginov, H. Li, Yu A. Barnakov, D. Dryden, G. Nataraj, G. Zhu, C. E. Bonner, M. Mayy, Z. Jacob, E. E. Narimanov. "Controlling spontaneous emission with metamaterials." *Optics letters* 35 (11), pp. 1863-1865 (2010).
27. Y. Guo, C. Cortes, S. Molesky, Z. Jacob. "Broadband super-Planckian thermal emission from hyperbolic metamaterials." *Applied Physics Letters* 101 (13), p. 131106 (2012).
28. I. Iorsh, A. Poddubny, A. Orlov, P. Belov, Y. S. Kivshar. "Spontaneous emission enhancement in metal–dielectric metamaterials." *Physics Letters A* 376 (3), pp. 185-187 (2012).
29. H.G. Zeuthen, Sur les différentes formes des courbes planes du quatrième ordre, *Mathematische Annalen* 7, pp. 408–432 (1873)
30. — Gao, Wenlong, et al. "Topological photonic phase in chiral hyperbolic metamaterials." *Physical review letters* 114.3 (2015): 037402.
31. B. D. H. Tellegen, *Philips Res. Rep.* 3, 81 (1948)
32. Tretyakov, S. A., A. H. Sihvola, A. A. Sochava, and C. R. Simovski. "Magnetoelectric interactions in bi-anisotropic media." *Journal of Electromagnetic Waves and Applications* 12, no. 4 (1998): 481-497.
33. C. Rüter, K. G. Makris, R. El-Ganainy, D. N. Christodoulides, M. Segev, and D. Kip. "Observation of parity–time symmetry in optics." *Nature Physics* 6 (3), pp. 192-195 (2010)
34. Bliokh, Konstantin Y., Yuri S. Kivshar, and Franco Nori. "Magnetoelectric effects in local light-matter interactions.", *Physical review letters* 113 (3), pp. 033601 (2014)
35. Lindell et al., *Plane-wave propagation in extreme magnetoelectric media*. *IEEE Transactions on Antennas and Propagation*, Vol. 64, No. 12, pp. 5382-5392, December 2016
36. Thomas Mulkey, Jimmy Dillies, and Maxim Durach, "Inverse problem of quartic photonics," *Opt. Lett.* 43, 1226-1229 (2018)
37. Reed Hodges, Cleon Dean, and Maxim Durach, "Optical neutrality: invisibility without cloaking," *Opt. Lett.* 42, 691-694 (2017)
38. X. Zhou and G. Hu, *Phys. Rev. E* 74, 026607 (2006)

**Table A.**

A	$-p_{26} + p_{35} + p_{53} - p_{62}$
B	$p_{12} + p_{21} + p_{45} + p_{54}$
C	$p_{13} + p_{31} + p_{46} + p_{64}$
E	$p_{16} - p_{34} - p_{43} + p_{61}$
F	$-p_{15} + p_{24} + p_{42} - p_{51}$
G	$p_{23} + p_{32} + p_{56} + p_{65}$
H	$p_{11} + p_{44}$
J	$p_{22} + p_{55}$
K	$p_{33} + p_{66}$